Magnetism in Nanocrystalline Gold

Vladimir Tuboltsev,[†,*] Alexander Savin,[‡] Alexandre Pirojenko,[†] and Jyrki Räisänen[†]

[†]Division of Materials Physics, Department of Physics, University of Helsinki, P.O. Box 43, FI-00014 Helsinki, Finland and [‡]O.V. Lounasmaa Laboratory, Aalto University School of Science, P.O. Box 15100, FI-00076 Aalto, Finland

ABSTRACT While bulk gold is well known to be diamagnetic, there is a growing body of convincing experimental and theoretical work indicating that nanostructured gold can be imparted with unconventional magnetic properties. Bridging the current gap in experimental study of magnetism in bare gold nanomaterials, we report here on magnetism in gold nanocrystalline films produced by cluster deposition in the aggregate form that can be considered as a crossover state between a nanocluster and a continuous film. We demonstrate ferromagnetic-like hysteretic magnetization with temperature dependence indicative of spin-glass-like behavior and find this to be consistent with theoretical predictions, available in the literature, based on first-principles calculations.

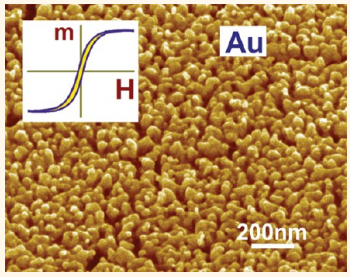

KEYWORDS: gold · nanocrystalline film · magnetism · cluster deposition · SQUID magnetometry

The continuously growing and centuries old attention to gold as a precious noble metal is due nowadays to the desire to develop new applications, devices, and products in nanoscience and nanotechnology employing new nanomotifs (nanoclusters, nanowires, nanofilms, nanostructured surfaces, *etc.*) offering properties not available in the bulk. In focus are novel electronic, optical, catalytic, tribological, antibacterial, *etc.*, properties of dispersed or finely divided gold and nanostructured surfaces with large surface-to-volume ratios.[1−4] Enabling a variety of new, exiting, and marketable techniques ranging from sensing to applications in biomedicine and forensic sciences, nanostructuring allows reducing considerably the amount of used gold (and, hence, cost) without degrading or sometimes even enhancing the desired functionality.

Until recently, magnetism in gold was of little interest. The first publications on the nondiamagnetic response in surface-capped gold nanoparticles have triggered enormous interest.[8,15] Gold is well known to be the only metal having an endothermic oxygen chemisorption energy and, thus, be inert to surface oxidation.[5] Therefore, gold forms a model material offering the possibility to study para- and ferromagnetism stimulated by nanostructuring in fundamentally nonmagnetic materials (meaning diamagnetic) with minimal influence of the surface chemical state. The latter is critical for nanomaterials with a large fraction of atoms at the surface and interfaces. On the other hand, imparting gold with ferromagnetic properties, especially remanence, would add more functionalities to gold-based applications and devices gaining sensitivity to external magnetic fields. This would provide a sensing option to magnetic signal generating stimuli and more degrees of freedom in control and manipulating *via* magnetization switching, *e.g.*, control over local catalytic properties[3] and applications in biomedicine and therapeutics, which demand high biocompatibility (precise drug delivery and cancer targeting,[6] magnetic resonance imaging and hyperthermia,[2] magnetically activated gold nanoparticle-based sensors[7]).

At present, it seems to be accepted that gold nanoparticles just a few nanometers in size may exhibit paramagnetism, superparamagnetism, and even characteristic features of a ferromagnetic material (see recent review in ref 7 and references therein). Having consensus on this, the explanation remains vague and is still under debate. It is noteworthy that most of the experimental research of nanogold magnetism reported so far has been done on gold nanoparticles synthesized using various surface stabilizer molecules.

According to one point of view, dominating at present, gold nanoparticles and thin films exhibit a nondiamagnetic response and permanent magnetization only when capped with strongly binding molecules causing electronic modification to the

* Address correspondence to vladimir.tuboltsev@helsinki.fi.

Received for review March 11, 2013 and accepted July 6, 2013.

Published online 10.1021/nn401914b

TABLE 1. Summary of Magnetic Characteristics of Au Nanoparticles, Nanoclusters, and Thin Films Published in the Literature[a]

Experiment							
gold form	nanoparticle diameter or film thickness [nm]	preparation method	surface capping agent	saturation magnetization M_s [emu cm^{-3}]	remanence M_r [emu cm^{-3}]	coercivity H_c [Oe]	ref no.
NP[b]	1.4	LCM[f]	DT[i]	19	7	250—860	9
NP	1.8—2	LCM	thiol	2.6—1.5		30—100	27
NP	1.9	LCM	DT	96.5	7.7	190	11
NP	2	LCM	DT	1.7	0.08	90	37
NP	2—2.7	LCM	DT	45—4.8		80—170	12
NP	2—10	LCM	DT	2.1—0.4	0.03—0.2	44—80	14
NP	5	LCM	DT	0.2	0.02	250	10
NP	2.3	LCM	OT[j]	1.4	0.05	50	35
NP	1.9	LCM	$SC_8/SC_{11}COOH$	0.2			35
NP	2.1	LCM	TPP[k]	0.2—0.3	0.04—0.06	200—400	13
NP	2—15	LCM	THPC[l]	1.9—0.06	0.004—0.3	60—136	14
NP	2.5	LCM	PVP[n]	25			15, 18
F[c]	100	LCM	polyalanine	0.7—9.3			8
F	100	LCM	alkylthiol	2.7—7.3			8
NCF[d]	28	CBD[g]	no	10.5—12	1.6—2.3	57—100	this work
NCF	175	CBD	no	0.9—1.1	0.2—0.3	73—111	this work

gold form	nanoparticle diameter or film thickness [nm]	preparation method	surface capping agent	magnetic moment [emu cm^{-3}]	ref. no.
NP	1.41	LCM	TPP	diamagnetic	13
NP	1.9	LCM	PAAHC[m]	1.0 ferromagnetic	17
NP	2.5	LCM	ST[o]	0.4 paramagnetic	35
F	27	VD[h]	no	1.6 paramagnetic	23

First-Principles Simulations					
Gold form	Cluster Size (Diameter [nm])	Surface Capping Agent	magnetic moment [10^{-21} emu]	magnetic moment [emu cm^{-3}]	ref. no.
NC[e]	Au_{12}; Au_{13} (0.75)	no	37.1; 46.4	168.6; 210.7	21
NC	Au_6—Au_{147} (1.68)	no	46.4—9.3	210.9—3.75	19
NC	Au_{38} (0.92)	no	26.1—45.4	64.0—111.3	20
NC	Au_{68} (1.24)	no	26.5—45.4	26.6—45.5	20

[a] For comparison, original magnetization data are expressed in emu cm^{-3} assuming bulk gold density. [b] NP, nanoparticles. [c] F, films. [d] NCF, nanocrystalline films. [e] NC, nanoclusters. [f] LCM, liquid chemical method. [g] CBD, cluster beam deposition. [h] VD, vacuum deposition. [i] DT, dodecanethiol. [j] OT, octanethiol. [k] TPP, phosphine-chlorine-capped in the presence of triphenylphosphine. [l] THPC, tetrakis(hydroxymethyl)phosphonium. [m] PAAHC, polyallyl amine hydrochloride. [n] PVP, poly(*N*-vinyl-2-pyrrolidone). [o] ST, tiopronin, a synthetic thiol-containing biomolecule ($C_5H_9NO_3S$).

surface atoms, *e.g.*, by thiol molecules.[8—12] Magnetization values as high as $\sim 2.78 \times 10^{-21}$ emu per surface Au atom have been reported.[11] Recent studies, however, indicate that the presence of strongly binding molecules on the surface is not the only nor a sufficient condition required for the induction of a ferromagnetic response, as was demonstrated, for example, in thiol-stabilized Au nanoparticles.[13,14] It is noteworthy that none of the published papers reporting on ferromagnetism in gold nanoparticles induced by surfactants provide a comparison with their bare counterparts, at least for reference.

Others believe that the observed departure from bulk diamagnetism is an intrinsic property of nanosized gold with large surface-to-volume ratio, and, on the contrary, weakly coupling surface agents are a prerequisite for ferromagnetism in gold nanoparticles.[15—18] Computer simulations also predict size-dependent spin polarization and ferromagnetism in bare gold nanoparticles and thin films due to the effect of surfaces at the nanoscale and strong spin—orbit coupling in gold.[19—22] Estimated magnetization values are on the same order of magnitude as those resulting from strongly binding capping molecules. Table 1 presents a summary of magnetic properties of gold nanoparticles, nanoclusters, and thin homogeneous and nanocrystalline films reported by different authors. The magnetic characteristics obtained experimentally are compared with those derived from the first-principles calculations. Counterintuitively, magnetic properties of bare gold nanomaterials are practically not studied experimentally, and information available in the literature is scarce.[23]

In the present work we employed the cluster beam deposition (CBD) technique to produce bare gold nanocrystalline films of size-selected clusters.[24,25] The films' magnetic properties were evaluated using ultra-high-sensitive magnetometry based on a superconducting quantum interference device (SQUID). Special attention was paid to the purity in experiments so that the results are not compromised by parasitic magnetic

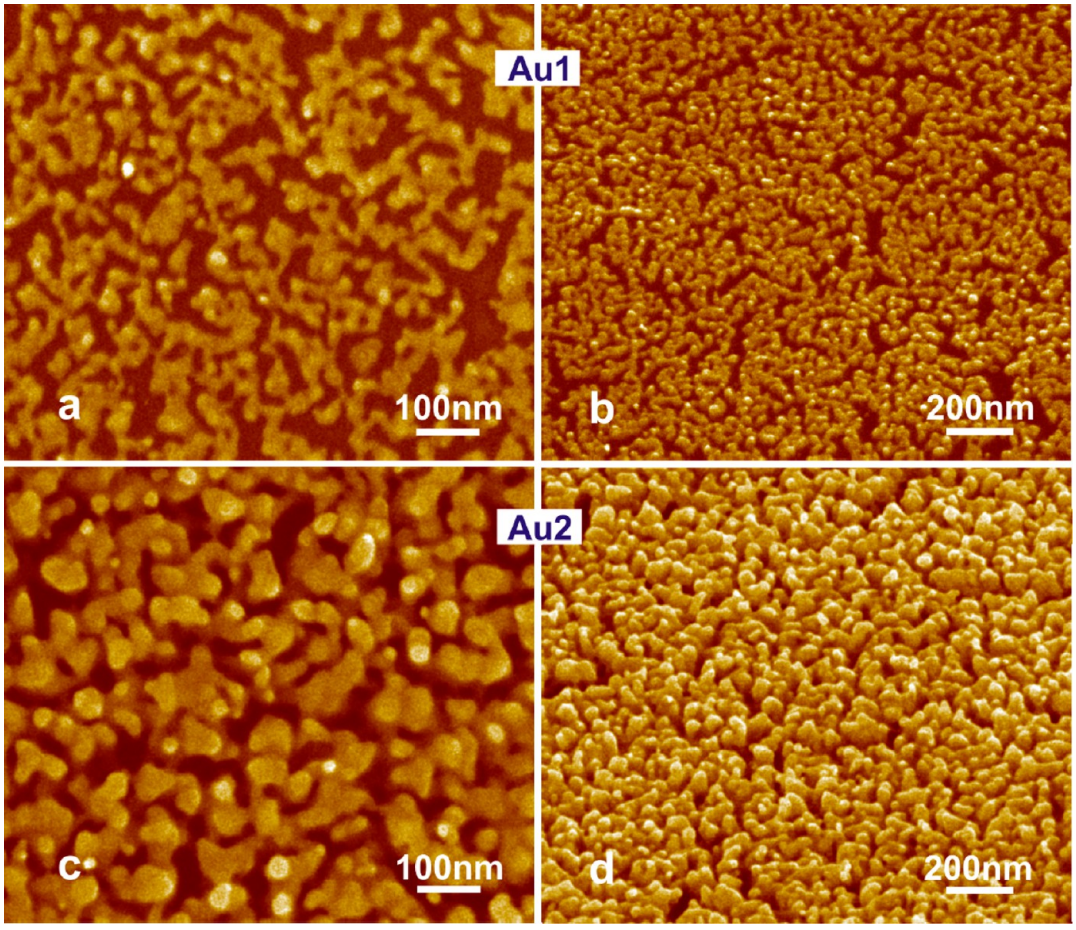

Figure 1. SEM micrographs of gold nanocrystalline films produced by cluster deposition in two aggregate states: Au1, fragmentary morphology of interconnected gold aggregates (a, b), and Au2, coral-motif agglomeration with highly developed effective surface (c, d).

impurities in both the deposited gold films and substrates (see Methods for details). With all the precautions taken we are confident that the total concentration of all trace elements in the gold films was at a level of 10 ppm.

RESULTS AND DISCUSSION

Figures 1 and 2 show scanning electron microscopy (SEM) and atomic force microscopy (AFM) micrographs of two selected deposited gold films. The films are seen to differ in their morphologies. The film Au1 shown in Figures 1(a,b) and 2(a) was formed by lower fluence cluster deposition. As one can see, the film has a fragmentary morphology with gold branches or aggregates interconnected in a quasi-percolation limit. The Au aggregates grow in the direction normal to the surface well before the continuous layer is formed. From Figure 1(b) it might appear that the film is built of round-shaped particles ~10 to 30 nm in size. However, the average size of Au clusters in the flux generated by our cluster source is $\sim 2.6 \pm 0.6$ nm (see Figure 3). The particular structure of the developed fragmentary, quasi-two-dimension lamellar layer is a result of partial cluster coalescence and coarsening on the surface unavoidable at the temperature of deposition. Figure 4 shows high-resolution transmission electron microscopy (HRTEM) images of gold aggregates deposited with a fluence half that used for Au1 and otherwise under the same conditions (see Methods section for details). Higher fluence deposition resulted in a quasi-three-dimensional coral-shaped film with a well-developed effective surface (Au2 in Figures 1(c,d) and 2(b)). The height of the gold agglomerates that can be considered as the film thickness was measured to be on average 28 and 175 nm, respectively, for Au1 and Au2 (see height diagrams in Figure 2). The total volume of gold confined in Au1 and Au2 was estimated to be 1.35×10^{-6} and 8.44×10^{-6} cm^3, correspondingly.

In Figure 5 magnetization *versus* applied magnetic field is shown for the selected films at different temperatures. Measurements at 1.8 and 400 K were done after cooling/heating in a zero magnetic field. Unlike the weak paramagnetic response observed in continuous gold films,[23] the magnetization in the nanocrystalline films is seen to exhibit characteristic ferromagnetic hysteresis with the coercive field (H_c), remanent (M_r), and saturation (M_s) magnetizations only slightly changing with temperature (see Figure 6).

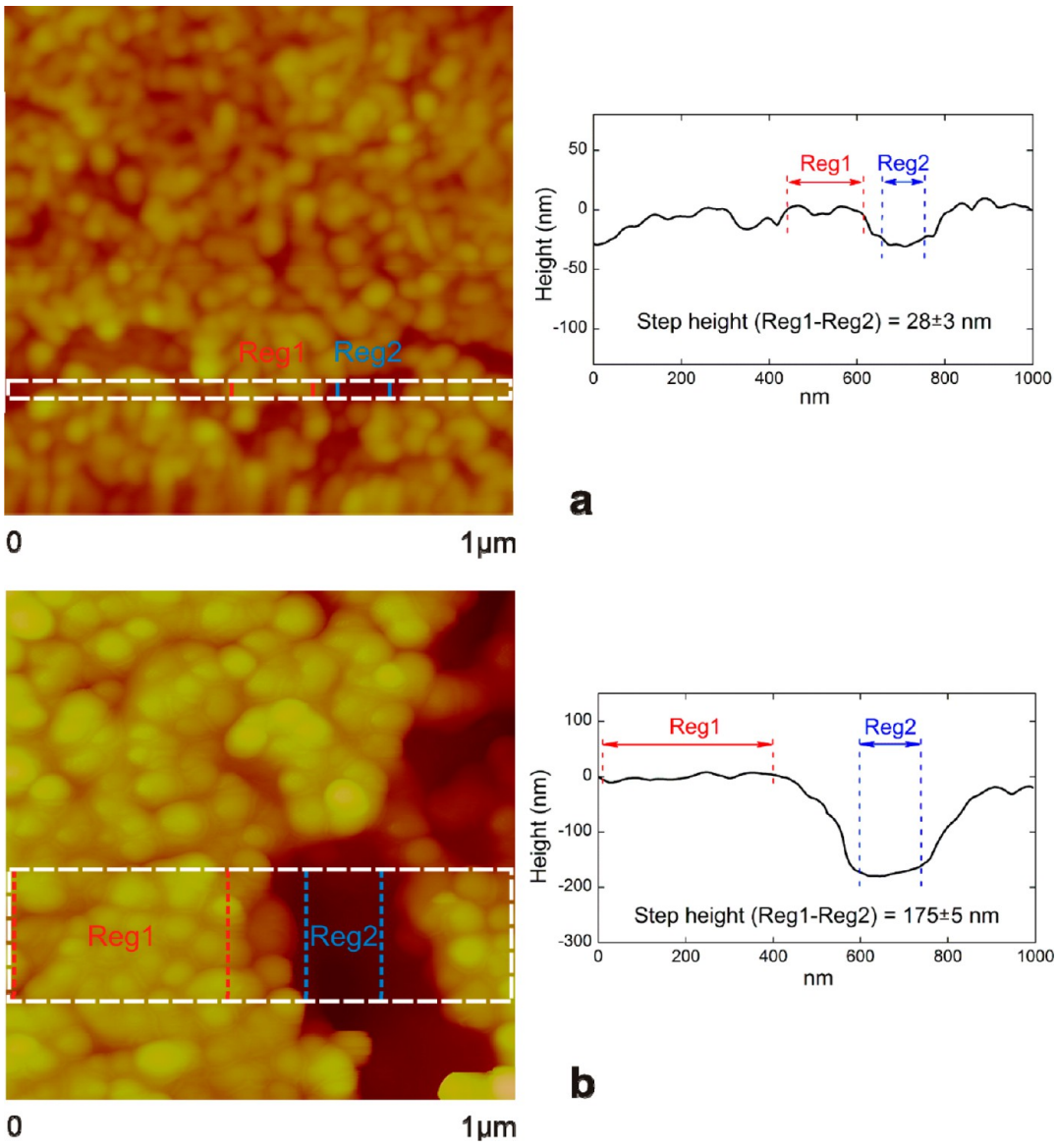

Figure 2. AFM topography images of gold nanocrystalline films Au1 (a) and Au2 (b) produced by low-energy cluster deposition. Gold features appear somewhat larger than in the SEM micrographs (Figure 1) due to the tip-convolution problem unavoidable in AFM imaging.

Though both coercivity and remanence decreased a little upon heating, the hysteresis in the magnetization is seen in Figure 5 to persist up to a temperature as high as 400 K. One may expect hysteretic magnetization even at higher temperatures; however, in our case 400 K was the maximum provided by our magnetometer. The error bars are not shown in Figure 5 for the sake of clarity. However, the experimental error in $m(H)$ measurements was $\sim 10^{-2}$ emu/cm^3, and, hence, the hysteresis could be unambiguously identified even at 400 K.

As it follows from Figure 5, the magnetization in Au1 exhibits saturation with a barely noticeable diamagnetic trend in the strong magnetic fields, the latter, however, being within the experimental scatter of the data points. One may suspect that the observed nondiamagnetic response is due to uncontrolled magnetic impurities in the gold. If we assume that all of the impurities are magnetic, say, Fe atoms, then the detected 10 ppm concentration would correspond to a magnetic moment of Fe as high as $\sim 2.4 \times 10^{-17}$ emu/atom, the latter being calculated from the saturation magnetization of Au1 at 1.8 K. The estimated value is unrealistically large when compared with magnetic moments of both free Fe atoms (2.06×10^{-20} emu) and those embedded into a Au matrix ($\sim 2.78 \times 10^{-20}$ emu).[26] Besides, Fe impurities were shown experimentally to actually weaken the ferromagnetic behavior in capped Au nanoparticles.[27] Therefore, the amount of possible magnetic impurities is definitely not sufficient to account for the magnetization values measured in the gold films.

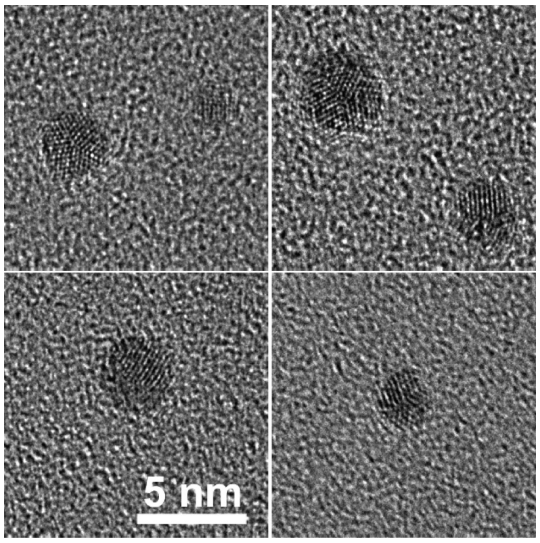

Figure 3. High-resolution TEM images of gold nanoclusters produced by the cluster beam source employed in fabrication of nanocrystalline films Au1 and Au2.

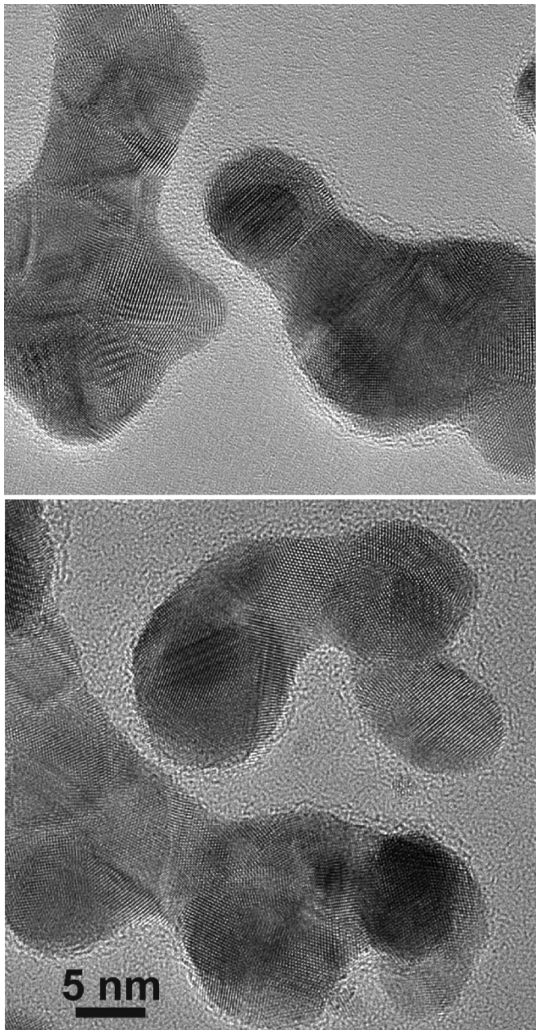

Figure 4. HRTEM micrographs of cluster-assembled Au aggregates with morphology exhibiting interfaces between nanocrystalline gold fragments formed by partial coalescence of deposited clusters and coarsening.

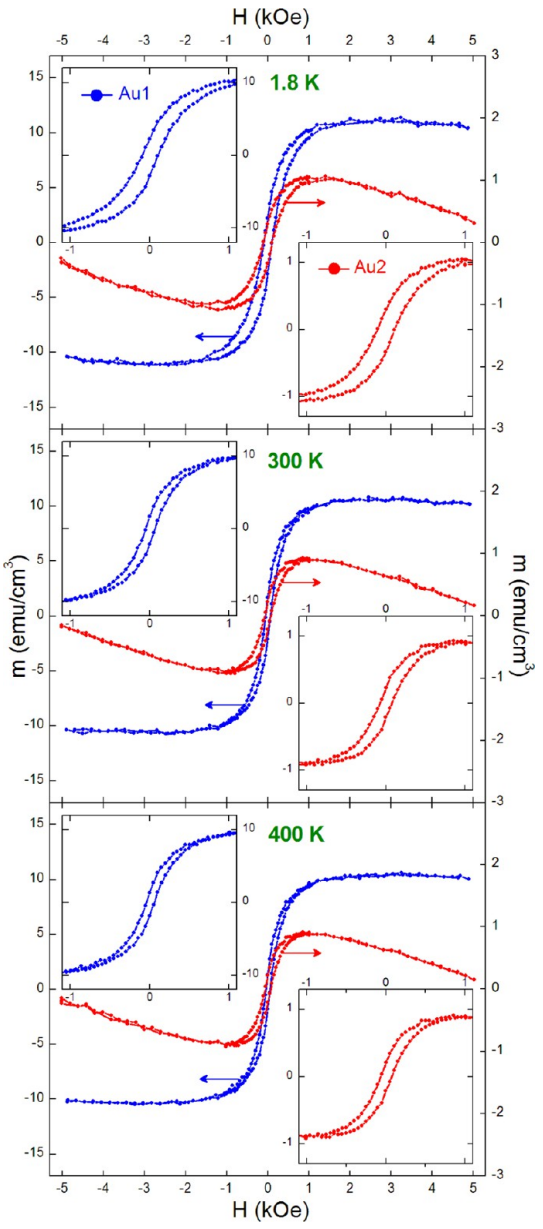

Figure 5. Magnetization of the cluster-deposited gold films Au1 (against the left axis) and Au2 (against the right axis) as a function of magnetic field measured at different temperatures. In the insets detailed views of the central parts of the hysteresis loops are shown.

The negative slope in the magnetization loop for Au2 in Figure 5 indicates the onset of the diamagnetism superimposed on the ferromagnetic hysteresis. This qualitatively different behavior manifests a transition to a new state exhibiting properties more pertinent to bulk gold. This is a nice example of how cluster deposition can be employed for synthesis of nanocrystalline materials with properties differing from those of the bulk. The morphology, structure, and properties of thin films made from deposited clusters are known to depend on a number of factors including the chemical nature of the elements involved, temperature, and impact energy of the clusters.[25] At low energies, the

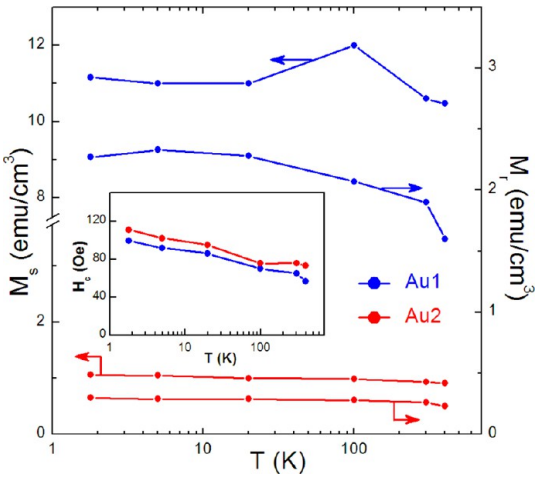

Figure 6. Temperature dependence of the saturation magnetization M_s, remanence M_r, and coercivity H_c for the cluster-deposited nanocrystalline gold films Au1 and Au2.

TABLE 2. Ratio of Surface and Volume Parameters for the Cluster-Deposited Gold Films Au1 and Au2

$S_{Au2}^{con}/S_{Au1}^{con}$ [a]	S_{Au2}/S_{Au1} [b]	V_{Au2}/V_{Au1} [c]
1.6 ± 0.2	1.8 ± 0.2	6.3 ± 0.8

[a] S_{Aui}^{con} (i = 1,2), area of surface where gold is in contact with the substrate. [b] S_{Aui}, effective total surface area of gold including the interface with the substrate. [c] V_{Aui}, total volume of gold.

clusters land softly at the substrate. Suffering minor distortion, clusters build up structures on the surface exhibiting a memory effect of the properties ascribed to a particular agglomerate state of the clusters provided that their integrity is preserved upon deposition. The energy of deposited Au clusters in our case was ~0.3 eV per atom. This corresponds to the low-energy regime of deposition, leading to formation of well-developed branches and porous-like morphology of the resulting films consisting of clusters as building blocks landing softly on top of each other and undergoing minor agglomeration.[25] In this regime the equilibrium film structure is determined mainly by the cluster surface mobility and thermodynamics of the cluster interaction rather than ballistic factors related to the impact energy. As a result, the intrinsic magnetic properties of Au clusters are more enhanced in the film Au1 and to a lesser extent in Au2, the latter having a higher volume fraction (see Table 2) and, hence, exhibiting more bulk-like properties (diamagnetism).

Although available theoretical models predicting and explaining the positive magnetization and ferromagnetism in bare gold nanoparticles differ in details, the common denominator is the existence of a core–shell magnetic structure with a bulk-like diamagnetic core and a shell of differently ordered surface magnetic moments.[19–22] The latter is caused by the reduced coordination of the surface atoms and strong spin–orbit coupling in gold. As a result, despite the filled d shells, Au

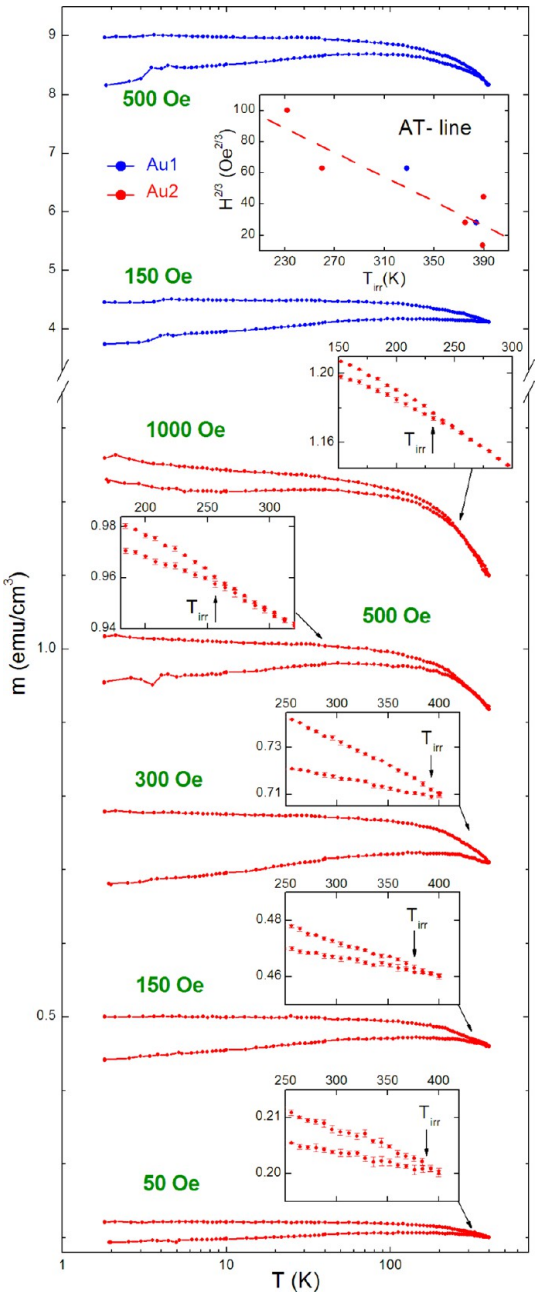

Figure 7. Temperature dependence of magnetization for the nanocrystalline gold films Au1 and Au2 measured after zero field cooling (lower branches of each curve) and cooling in different magnetic fields (upper branches). Top inset: Almeida–Thouless (AT) fit $H^{2/3} \propto T_{irr}$ to the experimental temperatures T_{irr} at which ZFC and FC curves for Au2 split in different magnetic fields. Two points for Au1 are shown just for comparison and were not used in the AT fit.

nanoclusters possess ground-state magnetic moments with spin-aligned electrons being itinerant on the outer shell of the surface atoms. These considerations suggest that the films produced in this work by cluster deposition in a quasi-null-coalescence regime can be considered as an assembly of interacting Au nanoclusters with the core–shell magnetic structure and positive magnetization confined to the shell. One striking conclusion following from Figure 5 is that the saturation magnetization of

Au1 is a factor of 10 greater than that of Au2 (after subtraction of the diamagnetic contribution). This cannot be explained only by the difference in the volume and effective surface atomic fractions. Table 2 shows surface and volume parameters estimated from the film analysis by electron and scanning probe microscopy. From Au1 to Au2 the amount of gold by volume has increased by a factor of 6.3, whereas the effective surface fraction, only by 1.8. If the ferromagnetism in the films is associated with the surface atoms and the diamagnetic contribution with the volume, then the morphological changes are not fully consistent with the 10-fold decrease in magnetization. However, the effective surface ratio in Table 2 was derived from the surface topography imaging, providing no information about the interfaces between Au nanoclusters and aggregates. Therefore, the real integral fraction of atoms on the surface and interfaces exhibiting positive magnetization and the nondiamagnetic response is assumed to be large due to the low impact energy of deposited clusters. This has particular relevance to the Au1 film. Diamagnetism was positively identified in the Au2 film, but not in Au1. This implies that higher fluence deposition reducing the distance between deposited Au aggregates and branches favors coalescence and leads eventually to the appearance of the phase in Au2 that can be considered as bulk-like.

Magnetization curves shown in Figure 5, virtually independent of temperature, suggest that the magnetization process in the films bears no relation to superparamagnetism when magnetic nanoparticles behave as nanosized ferromagnets. The core–shell magnetic structure of the Au clusters and aggregates composing the films is indirectly supported by the magnetization temperature dependence presented in Figure 7.

After cooling to the terminal temperature ~1.8 K in zero magnetic field, magnetization was measured as a function of temperature up to ~400 K in different applied magnetic fields (ZFC). Then, measurements continued while cooling back to the terminal temperature (FC). Unlike magnetic susceptibility of continuous gold films following the Curie-Weiss law,[23] the magnetization in our nanocrystalline films was found to exhibit irreversibility between ZFC and FC branches in all applied fields. After cooling in zero field, the magnetization goes through a broad maximum spanning from cryogenic temperatures to ~400 K. The temperature at which the curves split (T_{irr}) corresponds to the onset of the irreversibility. T_{irr} is seen in Figure 7 (top inset) to follow the Almeida–Thouless line $H^{2/3} \propto T_{irr}$, which might suggest a long-range spin-glass state and mean field system.[28] The temperature dependence is reminiscent of magnetization behavior in nanoparticle assemblies and nanocrystalline materials characterized by nanoparticulate morphology and a core–shell magnetic structure and referred to as spin-glasses, *e.g.*, strongly interacting ferromagnetic nanoparticles, antiferromagnetic oxides, and ferrites.[29–31] Spin-glass conventionally refers to magnetic spin systems with frustrated interactions between differently ordered spin subsystems and exhibiting multiple metastable states due to multiple minima in the corresponding energy landscape.[32] Behaving nonergodically below certain freezing temperature, the system is pinned to the local energy minimum and is not able to escape. We suggest that the core–shell structure and nanocrystalline morphology affect the magnetic properties of our nanocrystalline gold films. Temperature-dependent spin disorder at the surface/interface of the nanoparticles and nanoaggregates extending into the interior is believed to introduce magnetic frustration, in particular in Au1. The observed spin-glass collective state is assumed to be a complex interplay between surface and finite size effects associated with the spatial confinement, interparticle interactions, and the random anisotropy axis distribution.

CONCLUSIONS

Gold nanocrystalline films with nontrivial morphology and magnetic properties have been synthesized by low-energy cluster deposition. Through the careful control of parasitic magnetic impurities and avoiding using substrates causing an undesirable strong background signal, we present, in our opinion, convincing evidence of ferromagnetism intrinsic to bare gold in the nanocrystalline form. The findings are consistent with theoretical predictions available in the literature. Observed for the first time, anomalous temperature dependence of magnetization in nanocrystalline gold with particulate morphology suggests the existence of a spin-glass-like collective state that persists within a wide range of temperatures from cryogenic to well above room temperature.

METHODS

The gold clusters were produced using an NC200 (Oxford Applied Research) gas aggregation cluster source charged with a gold target of 99.999% purity (Kurt J. Lesker). Clusters in the source are formed through supersonic expansion of an Ar buffer gas containing gold atoms when traveling through a small nozzle from relatively high to lower pressure regions. Exchanging energy in collisions with other atomic species, the clusters eventually reach a velocity that is close to that of the expanding gas.[33] Hence, the cluster velocity V_c and kinetic energy E_c can be estimated as follows:[34]

$$V_c = (\gamma/(\gamma - 1))^{1/2}(2k_BT/M_g)^{1/2} \quad (1)$$

$$E_c = 0.5NM_cV_c^2 \quad (2)$$

where γ is the heat capacity ratio C_p/C_v equal to 5/3 for a monatomic ideal gas, k_B is the Boltzmann constant, T and M_g are

the gas temperature and atomic weight, and N and M_c are the cluster size and atomic weight. Estimations using eq 2 give ~0.3 eV/atom for the energy of the Au clusters produced in our experiments at room temperature.

By using the cluster deposition technique instead of employing surfactant chemical methods, the number of preparation steps was minimized; no strong solvents or acids and no extensive use of glassware and complex chemicals were involved. This reduced to minimum the risk of contamination, as even using Pyrex glassware may lead to unwanted magnetic impurities, *e.g.*, Fe.[35] It should be mentioned that our cluster deposition facility has never been used with any strong magnetic material, such as Co, Ni, or Fe, that could cause cross-contamination and unwanted impurities in the gold films. We took utmost care to avoid accidentally introducing magnetically active contaminants at all stages of sample preparation, manipulation, and analysis. The films were deposited at room temperature in ultrahigh-vacuum conditions in a chamber evacuated by an oil-free pumping system. During the deposition, the time of actual deposition was monitored while keeping all other experimental parameters the same for all the samples.

Magnetization measurements were performed using a SQUID magnetometer (Quantum Design MPMS-XL7), providing a magnetic field up to 70 kOe at temperatures from 1.8 to 400 K. The technique is integral and does not provide element selectivity in measurements on samples with analyzed material deposited on a substrate, typically quartz or silicon. Therefore, in order to avoid uncontrolled magnetic impurities associated with the substrates and strong bulk diamagnetic background, as well as possible influence of the surface silicon oxide,[36] the gold clusters were deposited directly on the lightweight homogeneous plastic straw provided by Quantum Design as a sample holder for ultrahigh-sensitivity measurements (part number AGC2). Each film was deposited on a section cut from the straw (~5 mm wide) that was used as a substrate. The measurements were performed in the sample vibrating mode, varying set parameters and using different algorithms supported by the magnetometer in order to ensure reproducibility and avoid any ambiguity in the interpretation caused by instrument-related artifacts. Since the level of magnetic response from the gold films was expected to be rather low, a possible parasitic background signal caused by the substrate shape, local deformations, material defects, and nonhomogeneity was evaluated before the deposition. The process of characterizing the magnetic substrate and removing parasitic noise involved performing the measurements with the virgin substrate (with no gold deposited) in place, but with all other experimental conditions configured as in the actual measurements. The resulting data were stored for subtraction from the actual magnetization data measured on the precharacterized substrates with deposited gold films.

The level of impurities in the gold films has been evaluated by inductively coupled plasma (ICP) mass spectrometry and elastic recoil detection (ERD) analysis after magnetization measurements. While the former is in general qualitative, yet extremely sensitive to trace elements, the latter is a self-calibrating quantitative technique having, on the other hand, a moderate sensitivity. The total concentration of all trace elements in the films was assured by the analytical techniques to be at a level of 10 ppm (see Supporting Information).

The films' morphology was examined by scanning electron microscopy employing a dual-beam focused ion beam (FIB) instrument (FEI Helios NanoLab 600), high-resolution transmission electron microscopy (JEOL JEM-2200FS), and atomic force microscopy (Veeco AutoProbe CP-Research). After magnetization measurements the samples were analyzed by SEM and AFM. For high-resolution transmission electron microscopy gold clusters were deposited on carbon holey films ~12 nm thick (Quantifoil Micro Tools GmbH). Since both Quantifoil carbon and the material of the plastic straw used in magnetization measurements are chemically inert, we assume that the morphology of the deposited gold films was not affected by the substrates.

Conflict of Interest: The authors declare no competing financial interest.

Supporting Information Available: Trace element analysis of the gold nanocrystalline films and substrates. This material is available free of charge *via* the Internet at http://pubs.acs.org.

Acknowledgment. The authors are grateful to Drs. K. Mizohata and H. Jiang for their help in characterizing our samples by ERD and HRTEM, respectively. This work has been supported in part by the Academy of Finland though its LTQ CoE grant (project no. 250280). Support from the Academy of Finland through projects 134406 and 263439 is acknowledged.

REFERENCES AND NOTES

1. Mohamed, A. A. Gold Is Going Forensic. *Gold Bull.* **2011**, *44*, 71–77.
2. Daniel, M. C.; Astruc, D. Gold Nanoparticles: Assembly, Supramolecular Chemistry, Quantum-Size-Related Properties, and Applications toward Biology, Catalysis, and Nanotechnology. *Chem. Rev.* **2004**, *104*, 293–346.
3. Bond, G. Source of the Catalytic Activity of Gold Nanoparticles. *Gold Bull.* **2010**, *43*, 88–93.
4. Turner, M.; Golovko, V. B.; Vaughan, O. P. H.; Abdulkin, P.; Berenguer-Murcia, A.; Tikhov, M. S.; Johnson, B. F. G.; Lambert, R. M. Selective Oxidation with Dioxygen by Gold Nanoparticle Catalysts Derived from 55-Atom Clusters. *Nature* **2008**, *454*, 981–983.
5. Hvolbæk, B.; Janssens, T. V. W.; Clausen, B. S.; Falsig, H.; Christensen, C. H.; Nørskov, J. K. Catalytic Activity of Au Nanoparticles. *Nano Today* **2007**, *2*, 14–18.
6. Jain, P. K.; El-Sayed, I. H.; El-Sayed, M. A. Au Nanoparticles Target Cancer. *Nano Today* **2007**, *2*, 18–29.
7. Trudel, S. Unexpected Magnetism in Gold Nanostructures: Making Gold Even More Attractive. *Gold Bull.* **2011**, *44*, 3–13.
8. Carmeli, I.; Leitus, G.; Naaman, R.; Reich, S.; Vager, Z. Magnetism Induced by the Organization of Self-Assembled Monolayers. *J. Chem. Phys.* **2003**, *118*, 10372–10375.
9. Crespo, P.; Litrán, R.; Rojas, T. C.; Multigner, M.; de la Fuente, J. M.; Sánchez-López, J. C.; García, M. A.; Hernando, A.; Penadés, S.; Fernández, A. Permanent Magnetism, Magnetic Anisotropy, and Hysteresis of Thiol-Capped Gold Nanoparticles. *Phys. Rev. Lett.* **2004**, *93*, 087204–087207.
10. Dutta, P.; Pal, S.; Seehra, M. S.; Anand, M.; Roberts, C. B. Magnetism in Dodecanethiol-Capped Gold Nanoparticles: Role of Size and Capping Agent. *Appl. Phys. Lett.* **2007**, *90*, 213102–213104.
11. Garitaonandia, J. S.; Insausti, M.; Goikolea, E.; Suzuki, M.; Cashion, J. D.; Kawamura, N.; Ohsawa, H.; Gil de Muro, I.; Suzuki, K.; Plazaola, F.; *et al*. Chemically Induced Permanent Magnetism in Au, Ag, and Cu Nanoparticles: Localization of the Magnetism by Element Selective Techniques. *Nano Lett.* **2008**, *8*, 661–667.
12. Garitaonandia, J. S.; Goikolea, E.; Insausti, M.; Suzuki, M.; Kawamura, N.; Osawa, H.; Gil del Muro, I.; Suzuki, K.; Cashion, J. D.; Gorria, C.; *et al*. Thiol-Capped Ferromagnetic Au Nanoparticles Investigated by Au L3 X-ray Absorption Spectroscopy. *J. Appl. Phys.* **2009**, *105*, 07A907–07A909.
13. Muñoz-Márquez, M. A.; Guerrero, E.; Fernández, A.; Crespo, P.; Hernando, A.; Lucena, R.; Conesa, J. C. Permanent Magnetism in Phosphine- and Chlorine-Capped Gold: From Clusters to Nanoparticles. *J. Nanopart. Res.* **2010**, *12*, 1307–1318.
14. Maitra, U.; Das, B.; Kumar, N.; Sundaresan, A.; Rao, C. N. R. Ferromagnetism Exhibited by Nanoparticles of Noble Metals. *ChemPhysChem.* **2011**, *12*, 2322–2327.
15. Hori, H.; Teranishi, T.; Nakae, Y.; Seino, Y.; Miyake, M.; Yamada, S. Anomalous Magnetic Polarization Effect of Pd and Au Nanoparticles. *Phys. Lett. A* **1999**, *263*, 406–410.
16. Hori, H.; Yamamoto, Y.; Iwamoto, T.; Miura, V.; Teranishi, T.; Miyake, M. Diameter Dependence of Ferromagnetic Spin Moment in Au Nanocrystals. *Phys. Rev. B* **2004**, *69*, 174411–174415.
17. Yamamoto, Y.; Miura, T.; Suzuki, M.; Kawamura, N.; Miyagawa, H.; Nakamura, T.; Kobayashi, K.; Teranishi, T.; Hori, H. Direct Observation of Ferromagnetic Spin Polarization in Gold Nanoparticles. *Phys. Rev. Lett.* **2004**, *93*, 116801–116804.
18. Yamamoto, Y.; Hori, H. Direct Observation of the Ferromagnetic Spin Polarization in Gold Nanoparticles. *Rev. Adv. Mater. Sci.* **2006**, *12*, 23–32.

19. Luo, W.; Pennycook, S. J.; Pantelides, S. T. s-Electron Ferromagnetism in Gold and Silver Nanoclusters. *Nano Lett.* **2007**, *7*, 3134.
20. Magyar, R. J.; Mujica, V.; Marquez, M.; Gonzalez, C. Density-Functional Study of Magnetism in Bare Au Nanoclusters: Evidence of Permanent Size-Dependent Spin Polarization without Geometry Relaxation. *Phys. Rev. B* **2007**, *75*, 144421–144427.
21. Pundlik, S. S.; Kalyanaraman, K.; Waghmare, U. V. First-Principles Investigation of the Atomic and Electronic Structure and Magnetic Moments in Gold Nanoclusters. *J. Phys. Chem. C* **2011**, *115*, 3809–3820.
22. Okazaki, K.; Teraoka, Y. Magnetic Structures in Metallic Thin Films. *Surf. Sci.* **1999**, *433*−*435*, 672–675.
23. Reich, S.; Leitus, G.; Feldman, Y. Observation of Magnetism in Au Thin Films. *Appl. Phys. Lett.* **2006**, *88*, 222502–222504.
24. Palmer, R. E.; Pratontep, S.; Boyen, H.-G. Nanostructured Surfaces from Size-Selected Clusters. *Nat. Mater.* **2003**, *2*, 443–448.
25. Binns, C. Nanoclusters Deposited on Surfaces. *Surf. Sci. Rep.* **2001**, *44*, 1–49.
26. Frota-Pessôa, S. Pairs of 3d Impurities in Au: Local Moments and Exchange Coupling from First-Principles. *J. Magn. Magn. Mater.* **2001**, *226*−*230*, 1021–1023.
27. Crespo, P.; García, M. A.; Fernández Pinel, E.; Multigner, M.; Alcántara, D.; de la Fuente, J. M.; Penadés, S.; Hernando, A. Fe Impurities Weaken the Ferromagnetic Behavior in Au Nanoparticles. *Phys. Rev. Lett.* **2006**, *97*, 177203–177206.
28. de Almeida, J. R. L.; Thouless, D. Stability of the Sherrington-Kirkpatrick Solution of a Spin Glass Model. *J. Phys. A: Math. Gen.* **1978**, *11*, 983–990.
29. Labarta, A.; Battle, X.; Iglesias, O. From Finite-Size and Surface Effects to Glassy Behaviour in Ferrimagnetic Particles. In *Surface E*ffects *in Magnetic Nanoparticles*; Fiorani, D., Ed.; Springer-Science: New York, 2005; pp 105−140.
30. Park, T.-J.; Papaefthymiou, G. C.; Viescas, A. J.; Moodenbaugh, A. R.; Wong, S. S. Size-Dependent Magnetic Properties of Single-Crystalline Multiferroic $BiFeO_3$ Nanoparticles. *Nano Lett.* **2007**, *7*, 766–772.
31. Tuboltsev, V.; Savin, A.; Sakamoto, W.; Hieno, A.; Yogo, T.; Räisänen, J. Spin-Glass Behavior of Nanocrystalline Multiferroic Bismuth Ferrite Lead Titanate. *J. Mater. Chem.* **2011**, *21*, 781–788.
32. Fischer, K. H.; Hertz, J. A. *Spin Glasses*; Cambridge University Press: Cambridge, U.K., 1991.
33. Yamada, I.; Toyoda, N. Resent Advances in R&D of Gas Cluster Ion Beam Processes and Equipment. *Nucl. Instrum. Methods Phys. Res. B* **2005**, *241*, 589–593.
34. Anderson, J. B.; Fenn, J. B. Velocity Distributions in Molecular Beam from Nozzle Sources. *Phys. Fluids* **1965**, *8*, 780–787.
35. Grace, P. J.; Venkatesan, M.; Alaria, J.; Coey, J. M. D.; Kopnov, G.; Naaman, R. The Origin of the Magnetism of Etched Silicon. *Adv. Mater.* **2009**, *21*, 71–74.
36. Kopnov, G.; Vager, Z.; Naaman, R. New Magnetic Properties of Silicon/Silicon Oxide Interfaces. *Adv. Mater.* **2007**, *19*, 925–928.
37. Guerrero, E.; Muñoz-Márquez, M. A.; Guerrero, E.; Fernández-Pinel, E.; Crespo, P.; Hernando, A.; Fernández, A. Electron Structure, Magnetic Properties, and Microstructural Analysis of Thiol-Functionalized Au Nanoparticles: Role of Chemical and Structural Parameters in the Ferromagnetic Behaviour. *J. Nanopart. Res.* **2008**, *10*, 179–192.